Boron in wildfires: New insights into boron isotope fractionation during volatilisation, leaching and adsorption after combustion

Shawn Lu, Anthony Dosseto, Damien Lemarchand

Geochimica et Cosmochimica Acta 379 (2024) 208–218

Contents lists available at ScienceDirect

Geochimica et Cosmochimica Acta

journal homepage: www.elsevier.com/locate/gca

Boron in wildfires: New insights into boron isotope fractionation during volatilisation, leaching and adsorption after combustion

Shawn Lu [a,*], Anthony Dosseto [a], Damien Lemarchand [b]

[a] Wollongong Isotope Geochronology Laboratory, School of Earth, Atmospheric and Life Sciences, University of Wollongong, Keira Street, Wollongong, New South Wales 2522, Australia

[b] Institut Terre et Environnement Strasbourg (ITES), Université de Strasbourg-EOST, CNRS, ENGEES, 5 rue René Descartes, 67084, Strasbourg Cedex, France

ARTICLE INFO

Associate editor: Jiubin Chen

Dataset link: https://doi.org/10.17632/tgd5kj3wzk.2

Keywords:
Bushfire
Boron isotopes
Fire severity
Adsorption
Hysteresis

ABSTRACT

Wildfires are hazards of increasing significance in recent decades. Our ability to forecast the evolution of fire regimes is inhibited by the lack of records of key fire parameters such as fire severity. Boron isotopes in the soil clay fraction have been shown to vary with fire severity, where increased $\delta^{11}B$ coincides with higher fire severity. To elucidate the relationship between the B isotope composition of soil clays and fire events, we performed adsorption experiments by reacting rainwater with combusted leaves to analyse how B isotopes are fractionated during processes leading to the imparting of boron from plants to clay minerals in soil during and following combustion. We find that < 5% of B is volatilised during combustion of leaves and barks, where ^{11}B is preferentially volatilised. No isotopic fractionation was detected during the leaching of leaves ash with rainwater, possibly due to the large water:clay ratio in our experiments. Adsorption of B from leaching solutions onto clay minerals shows isotopic fractionation, and hysteresis of the adsorbed B fraction. For experiments at pH between 7 and 9, the isotope fractionation between adsorbed and dissolved B ($\Delta^{11}B_{adsorbed\text{-}dissolved}$) ranges from −8.8 to −14.5‰, indicating preferential adsorption of ^{10}B onto clays compared to ^{11}B. For experiments at pH > 10, the $\Delta^{11}B_{adsorbed\text{-}dissolved}$ values range from +11.2 to +19.4‰, indicating a preferential adsorption of ^{11}B over ^{10}B. Irregardless of pH, clay fractions in all experiments show increases in $\delta^{11}B$, as the leaching solutions have high $\delta^{11}B$ relative to the soil clay minerals prior to their interaction. Ash of leaves combusted at 550 °C (highest temperature in our experiments) induce the greatest increase in solution pH and $\delta^{11}B$ in clays. Our experiments suggests that the higher B isotope composition of clays following a high severity fire is likely imparted by solutions that leach isotopically heavy B from the combusted canopy.

1. Introduction

Boron (B) is a mobile trace element with two stable isotopes, ^{10}B and ^{11}B, and has a typical concentration of 20–200 mg/kg in soil (Mengel et al., 2001; Hu and Gao, 2008). Boron exists in solution as either $B(OH)_3$ or $B(OH)_4^-$, where due to their structures, the tetrahedral $B(OH)_4^-$ is enriched in ^{10}B, while the trigonal $B(OH)_3$ is enriched in ^{11}B (Kakihana et al., 1977). The influx of B in soils consists mainly of atmospheric input, chemical weathering of the parent material, and biogeochemical cycling (Schlesinger and Vengosh, 2016; Gaillardet and Lemarchand, 2018). The B biogeochemical cycle dominates the B flux in soil, and can range from 9.1 to 191 mg/m^2/yr (Cividini et al., 2010; Kot et al., 2016; Gaillardet and Lemarchand, 2018), which corresponds to being 1 to 3 orders of magnitude greater than atmospheric and mineral weathering B input. It has been suggested that the B biogeochemical flux varies by soil depth, with the B flux in the top 10 cm being 10 times greater than that of 30 cm depth (Cividini et al., 2010). If this B turnover is a semi-closed system consisting of B leaching from leaves and litter, and re-uptake of dissolved B by live plants, as shown in Kot et al. (2016), it could suggest that the residence time of dissolved B in the soil is not very long, as the dissolved B fraction do not have the opportunity to leach to deeper depths. This could possibly be due to a combination of fast B uptake by live plants and export of dissolved B by soil drainage (Roux et al., 2022). Since plants can only uptake soluble B, the biogeochemical B flux in the soil would be controlled by the B adsorption/desorption processes from soil solution.

Boron is a micronutrient that is essential for maintaining cell rigidity as well as plant growth and reproduction (Blevins and Lukaszewski, 1998; Dembitsky et al., 2002; Buoso et al., 2020). Plants can uptake B passively as boric acid from soil solutions with high B supply, where $B(OH)_3$ enters the root systems via diffusion, thus enriching the roots in ^{11}B relative to the soil solutions (Dembitsky et al., 2002; Miwa

* Corresponding author.
E-mail address: chl975@uowmail.edu.au (S. Lu).

https://doi.org/10.1016/j.gca.2024.04.024
Received 30 May 2023; Accepted 18 April 2024
Available online 24 April 2024

and Fujiwara, 2010; Geilert et al., 2019). In B-limited soils, plants can utilise active transport facilitated by proteins that preferentially uptake $B(OH)_4^-$, thus enriching the roots in ^{10}B relative to soil solutions (Geilert et al., 2019; Xiao et al., 2022; Chen et al., 2023). In some ecosystems, plants may not significantly fractionate B isotopes during root uptake, as one analysis of soil solutions at the depths of root activity show no significant difference in B isotope compositions to those of B input from throughfalls and litterfalls (Cividini et al., 2010). B isotopes are fractionated within plants themselves, where plant compartments show increased enrichment in ^{11}B with distance from the roots (Geilert et al., 2015, 2019; Roux et al., 2022; Xiao et al., 2022). For example, Geilert et al. (2015) reported average B isotope compositions of −11‰, −6.1‰, and 13.6‰ in bell pepper roots, stems and leaves, respectively. Similarly, Roux et al. (2022) found −11.7‰, 2.7‰, and 23.5‰ in the roots, stem and leaves of beech trees, respectively. The intra-plant B isotope fractionation can be explained by preferential incorporation of the lighter ^{10}B from the xylem sap into plant cells. This leads to a Rayleigh-like B isotope fractionation where the xylem sap and plant structures become increasingly enriched in ^{11}B the greater distance they are from the soil (Roux et al., 2022). Therefore, leaves from the canopy have heavier B isotope compositions than that of barks and lower branches.

Boron isotopes could possibly be used as a fire severity proxy, which could help resolve the lack of fire severity records required to model the impact of future wildfires on the environment (Lu et al., 2022). Because the B budget in the soil is largely controlled by biogeochemical cycling, disruptions to the ecosystem, such as those caused by wildfires, could affect the B composition in soil. High severity fires consume forest canopies, while low severity fires are confined to the understory and do not consume as much biomass. The combusted plant materials are deposited in soil as ash or charcoal, which can then contribute their B content to soil secondary minerals. The strong intra-plant B isotope fractionation could result in different B isotope signals in the soil between different fire severity. It has been shown that soil clay fractions from sites affected by high severity fires tend to have heavier B isotope composition to those that only experienced low severity fires (Lu et al., 2022). This fire signal can also be preserved in sediment records, where known fire events coincide with heavier B isotope compositions in the sediment layer (Ryan et al., 2023). Boron isotopes could therefore allow the reconstruction of fire severity variations of past wildfires over time, thus enabling more robust fire regime modelling. However, it is important to have better understanding of the processes leading to enrichment of ^{11}B in clay minerals following high severity fires. It is not entirely clear how B behaves during combustion of plant materials. It was shown that almost all the B in coal is recovered in ash after combustion, suggesting insignificant B volatilisation during combustion (Ochoa-González et al., 2011). On the other hand, it has been suggested that B volatilised during coal combustion could enrich the atmosphere with ^{10}B (Sakata et al., 2010), possibly increasing the B isotope signal to the soil if the volatilised B fraction is significant. Moreover, it is not known if significant B isotope fractionation occurs during volatilisation.

It is also crucial to understand the dynamics of B isotope fractionation both during, and after B is leached from combusted plants into soil solution. Boron is leached from coal ash at a faster rate at lower pH, although in conditions ranging from acidic to neutral pH, the rate of leaching is fast enough such that 15-mins of reaction time is enough to leach all water-leachable B into solution (Cox et al., 1978). At alkaline pH conditions, the B-leaching decreases linearly with increasing pH, ending in almost no B leached into solution at pH of around 11 after 24 h (Hollis et al., 1988). There is little information on how the isotope composition of the water-leached B fraction compares to that of the parent ash. Solution ^{10}B is generally preferentially sorbed onto clay minerals due to their surface structures having greater affinity for $B(OH)_4^-$ (which is enriched in ^{10}B relative to $B(OH)_3$). Keren and Mezuman (1981). However, solution pH could change the isotope fractionation during B adsorption, where increased pH leads to increased preferential adsorption of ^{11}B onto clays, humic acids and oxides (Palmer et al., 1987; Lemarchand et al., 2005, 2007). This is because at increased pH, $B(OH)_4^-$ becomes proportionally more abundant, leading to progressive enrichment of ^{11}B in $B(OH)_4^-$ (Palmer et al., 1987). Ash deposition can increase the soil pH following wildfires (Ulery et al., 1993), and could therefore influence both how B is leached into solution, and how it subsequently sorbs onto clay minerals.

This study aims to investigate how B isotopes are fractionated during and after wildfires as B is released from burnt vegetation and ultimately adsorbed onto clays. This would help explain the change in B isotope composition of soil clay fractions in response to fire severity observed in a previous study. To test if B volatilisation during combustion is significant, and whether it is accompanied by isotope fractionation, we measure the B concentration and isotope composition of plants before and after combustion. In addition, an adsorption experiment was conducted where B is leached from combusted leaves and reacted with clays. This is to test if combustion of isotopically heavier leaves could change the B isotope composition of clays in the same way to that observed in soil clay fractions affected by wildfires. This will be compared to results of a similar B leaching experiment using bark that was previously conducted (Lu et al., 2022), to verify the effect of intra-plant B isotope fractionation on B isotopes in the soil following wildfires.

2. Methods

2.1. Soil preparation

Soil was collected from the crest of Mt Keira in Wollongong (NSW, Australia). The bulk soil was wet sieved to obtain the < 63 μm fraction. This fraction was dried at 60 °C, then re-suspended in solution with 18.2 MΩ-cm water. About 250 mg of sodium hexametaphosphate was added for deflocculation. The mixture was then centrifuged following the protocol outlined in Starkey et al. (1984) to obtain the < 2 μm clay fraction. The clay fractions were rinsed repeatedly with ultrapure water, then freeze-dried. X-ray diffraction was used to identify the secondary mineral in the clay fractions, using a BRUKER-binary V3 (RAW) diffractometer at the University of Wollongong. Samples were analysed between 10 and 90° 2θ with a step size of 0.02 at 1° per minute.

2.2. Combustion of plant material

Eucalypt leaves and barks were collected from the same locations as the soil sample sites on Mt Keira. They were dried in the oven at 60 °C. The samples were cut into ~ 1 cm pieces and placed in ceramic crucibles for combustion in the muffle furnace. To test how combustion may change the B concentration and isotope composition, plants samples were combusted at 500 °C for 2 h, with a 30 mins ramp time. The resulting combustion residue was then digested (see below), and compared to aliquots of unburnt plant samples. Three replicates each of dried eucalypt leaves and barks were processed. Aliquots of these replicates were then combusted at 500 °C. For the leaching experiment, the leaves were combusted at 200, 300 and 550 °C instead. This produces a black residue at 200 and 300 °C, and a white ash at 550 °C. A loss on ignition (LOI) test was done by combustion at 500 °C for 5 h in a muffle furnace to measure the organic content of these combustion residues.

2.3. Boron leaching and adsorption experiment

Rainwater was collected in Wollongong (NSW, Australia), and filtered with 0.2 μm filter. This filtered rainwater will henceforth be referred to as Stage 1 solution (Fig. 1). About 0.22 g of combustion residue was added to 50 mL of Stage 1 solution, and left on a mixing

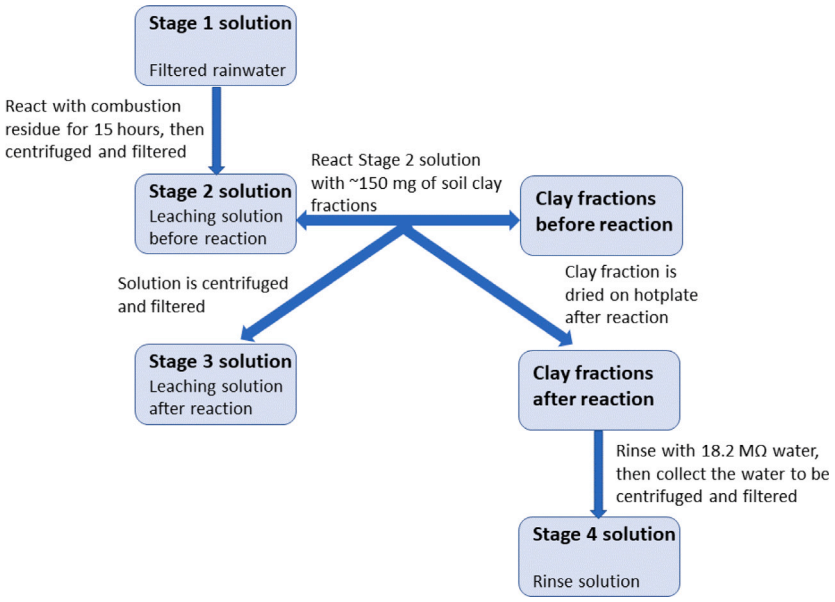

Fig. 1. A flowchart summary of the procedures for the B leaching and adsorption experiments.

wheel for 15 h at room temperature. The solutions were then centrifuged and filtered to remove the combustion residue. An aliquot of the resulting solution (henceforth referred to as Stage 2 solution) was taken for B concentration and B isotope measurements. Then, 12 mL aliquots of Stage 2 solutions were reacted with ~ 150 mg of clay (80: 1 water: clay ratio) fractions overnight. Following the reaction, the mixtures were centrifuged and aliquots of the supernatant solutions (henceforth referred to as Stage 3 solutions) were removed as much as possible with a pipette and collected for B concentration and B isotope measurements. The clays were then dried at 60 °C. Lastly, the clays were soaked with 10 mL of 18.2 MΩ-cm water overnight, then dried a final time after removing the solution as much as possible. Aliquotes of the soaking solutions (henceforth referred to as Stage 4 solutions) were also collected to measure the desorbed B. The entire experiment was repeated at 30:1 water: clay ratio, for combustion residue of leaves combusted at 200 °C, by adding ~ 200 mg of clay to 6 mL of Stage 2 solution, in order to test the effects of water: clay ratios.

2.4. Boron concentration and isotope analysis

2.4.1. Plant samples

Fresh plant samples were dried and ground to a fine powder, then added to a 1 M solution of 2/3 HNO_3 and 1/3 HCl, following the protocol outlined in Roux et al. (2015). The samples were left overnight to predigest, in order to prevent building up too much pressure in the digestion vessels. Complete digestion was then achieved using microwave-assisted digestion (with a MARS 6 microwave). The ramp time was 45 min, reaching a maximum temperature of 190 °C, where it was held for 90 min. Ash samples were digested with the same method. The solution was then loaded onto a cation exchange column filled with 1.5 mL of BIORAD AG50W-X8 resin. The resin was cleaned with 6 M HCl and conditioned with 0.01 M HCl. 5 mL of sample solution was loaded onto the column, followed by 2 mL of 0.01 M HCl to ensure complete sample recovery. Next, a microsublimation step is needed to remove the organic matter from the solution. The microsublimation protocol is adapted from Roux et al. (2015). First, a 0.5 mL aliquot was loaded onto the cap of a 15 mL PFA vial. The vial was then tightly closed upside-down, so that the solution stays on the cap. Aluminium foil was wrapped around the bottom and sides of the cap, then the vial was placed upside-down onto a hot plate, so that the bottom of the cap is in contact with the heating surface. The solution was heated at 110 °C for 3 h, then allowed to cool for 30 min. After the solution has cooled, the vial was carefully rotated to collect all the condensation droplets, while avoiding having the solution come into contact with the lid, where organic matter and silica have precipitated. The solution was then ready for chromatography (see below). Ash from combusted plant samples were digested following the same protocol.

2.4.2. Clay samples

Alkali fusion has been shown to be a reliable method to digest silicate materials for B analysis (Lemarchand et al., 2012; Lu et al., 2022). 50 mg of clay from the adsorption experiment was mixed with 250 mg of potassium carbonate (99.99% trace metal) in platinum (Pt)-gold (Au) crucibles (Pt-Au05). The mixture was heated at 950 °C for 40 min, and the resulting fusion residue was dissolved in 4 mL of 2 M HCl and sonicated. The solution was rapidly diluted to 40 mL with ultrapure water in a PP tube to minimise precipitation of Al and Si rich phases. The solution was centrifuged and a 5 mL aliquot of the supernatant was collected and loaded onto a cation exchange column filled with 1.5 mL of BIORAD AG50W-X8 resin, in order to remove the surplus potassium ion introduced during alkali fusion. The cation exchange resin used here was prepared with the same methods as in the plant sample section (see above). The eluted solution was then ready for chromatography (see below)

2.4.3. Boron chromatography

Boron was purified prior to analysis on a mass spectrometer, in a Class 100 cleanroom at Wollongong Isotope Geochornology Laboratory (WIGL). The leaching solutions from the adsorption experiments, the digested plant and ash samples, and digested clay samples all follow the same protocol from here, as adapted from Lemarchand et al. (2012). First, the pH of the sample solution was adjusted to 8–10, which was optimal for B adsorption on Amberlite resin, by adding purified 0.5 M NaOH. The solution was then loaded on 0.5 mL of B-specific Amberlite IRA 743 resin (100–200 mesh). The resin was cleaned with 0.5 M HCl and ultrapure water, and conditioned with ultrapure water. Matrix elements were eluted with 2.5 mL of ultrapure water, 2.5 mL of 0.5 M NaCl, and another 2.5 mL of ultrapure water. Finally, B was eluted with 5 mL of 0.5 M HCl and collected, ready for B concentration and isotope measurements.

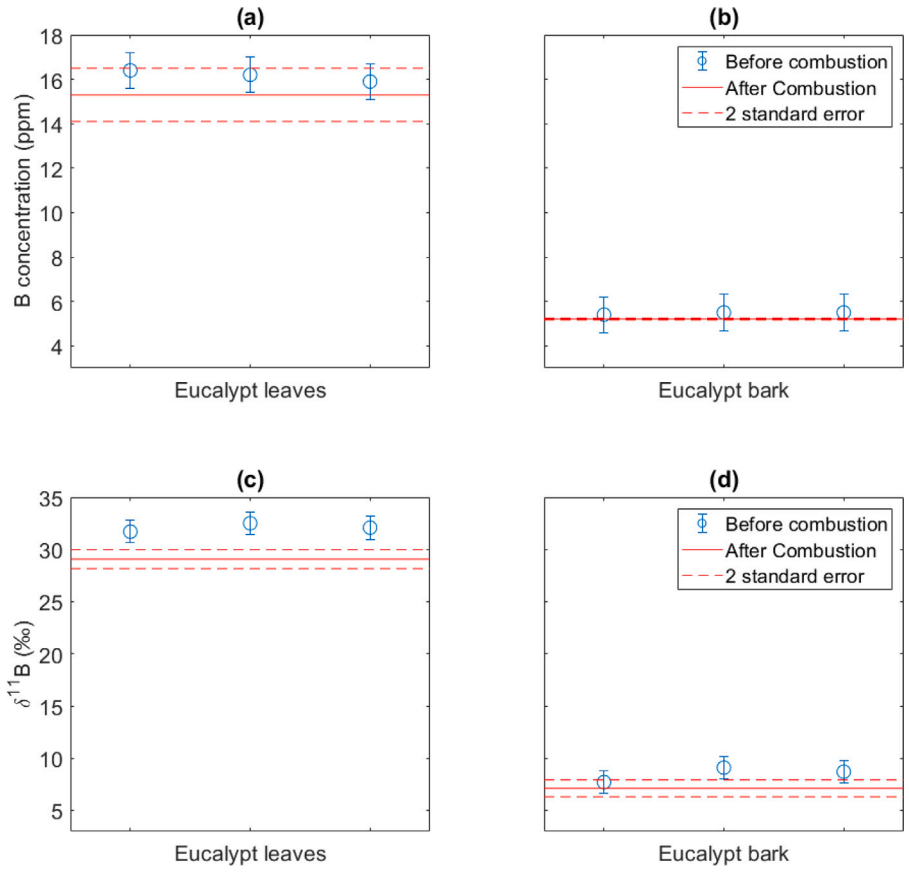

Fig. 2. B concentration (in ppm) of eucalypt leaves (a) and bark (b), as well as B isotope composition (in ‰) of eucalypt leaves (c) and bark (d), from Mt Keira (NSW, Australia), before and after being combusted at 500 °C. The red lines represent the mean and 2SE of three measurements for leaves and barks after combustion. For eucalypt bark after combustion (b), the 2SE is very small because the three replicates had very similar values.

2.4.4. Boron concentration and isotope measurements

Boron concentration and isotope measurements were carried out on a ThermoFisher Scientific Neptune Plus Multi-collector Inductively Coupled Plasma Mass Spectrometer (MC-ICP-MS) at WIGL. The sample introduction system consists of a dual cyclonic quartz spray chamber, standard nickel sample and skimmer cones, and an Apex PFA nebuliser with a flow rate of 100 μL min^{-1} (Elemental Scientific). Correction of mass bias was done by standard-sample bracketing using a 50 ppb solution of NIST SRM 951a as the primary standard. Background correction was done by measuring 0.5 M HCl as blanks before each standard and sample. The B isotopic compositions were expressed in δ^{11}B:

$$\delta^{11}B = \left[\frac{(^{11}B/^{10}B)_{sample}}{(^{11}B/^{10}B)_{NIST}} - 1\right] \times 1000 \quad (1)$$

where (^{11}B/^{10}B) refers to the B isotope ratio, and subscripts *sample* and *NIST* refer to the sample and the primary standard (NIST SRM 951a), respectively. Accuracy and precision during analysis were determined with 50 ppb solutions of ERM AE120 and AE121. The same batch of HCl used for sample elution was used for blanks, primary and secondary standard dilutions, in order to avoid mass bias caused by different acid matrices (Roux et al., 2015). We measured δ^{11}B values of −20.33±0.18‰ (2σ, n = 7) and 19.73±0.15‰ (2σ, n = 6) for AE120 and AE121, respectively. These values are within error of reported values of −20.2±0.6‰ and 19.9±0.6‰ for AE120 and AE121, respectively (Vogl and Rosner, 2012). Accuracy and precision of the entire protocol for processing clays and plants were determined by processing W-2a (USGS) and NIST SRM 1570a spinach leaves standards, respectively. We measured a δ^{11}B of 11.71 ± 1.09‰ (2 SE; n = 3) and 27.61 ± 0.27‰ (2 SE; n = 4) for W-2a and NIST SRM 1570a, respectively. This is similar to other studies which report a B isotope composition of 12.2±0.4‰ for W-2a (Ercolani et al., 2019; Gangjian et al., 2013), and 25.74 ± 0.21‰ to 26.1 ± 0.5‰ for NIST SRM 1570a (Roux et al., 2015; Wright et al., 2021).

The B concentration of the analyte solution was calculated by comparing the ^{11}B intensity of the solution to that of the 50 ppb primary standard used during isotope analysis (see above). The B concentration of the sample can then be calculated using the B concentration of the analyte solution, mass of the analyte solution, the solution loaded for chromatography, and that of digested sample. We measure a B concentration of 37.9 ± 0.8 ppm (2 SE; n = 4) for NIST SRM 1570a, which is in agreement with the certified value of 37.6 ± 1.0 ppm. For W-2a we measure a B concentration of 11.8 ± 0.7 ppm (2 SE; n = 3), which is in agreement with Govindaraju (1994), Ercolani et al. (2019) who reported a B concentration of 12.0 ± 0.3 ppm. The total procedural blank for plant digestions have 0.80 ± 0.02 (2 SE; n = 3) ng of B. For clay samples, one total procedural blank was processed and it had 2.2 ng of B.

3. Results

Both eucalypt leaves and barks have a narrow range of B concentrations and B isotope compositions (Figs. 2). For leaves, the mean B concentration is 16.2 ± 0.3 ppm (2 SE), and the mean B isotope composition is 32.10 ± 0.46‰ (2 SE; Table S2). For barks, the mean B concentration is 5.5 ± 0.1 ppm (2 SE), and the mean B isotope composition is 8.50 ± 0.82‰ (2 SE; Table S2). After being combusted, eucalypt leaves and barks display a B concentration of 15.3 ppm and 5.2 ppm, respectively (Fig. 2). This is within error of their respective B concentrations prior to combustion (Fig. 2). The average B isotope

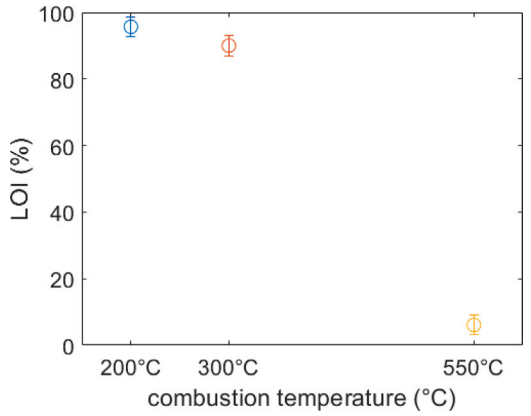

Fig. 3. LOI (%) of combustion residue for Eucalypt leaves combusted at 200, 300 and 550 °C. The mass fraction not lost during LOI is interpreted to be ash.

composition for eucalypt leaves is $29.07 \pm 0.29‰$ after combustion, which is ~3‰ lower than that before combustion; for eucalypt bark, the average B isotope composition after combustion is $7.12 \pm 0.29‰$, which is ~ 1.4‰ lighter than that before combustion (Fig. 2). For leaves, combusting at 200, 300 and 550 °C resulted in residues with LOI of 4.3, 10.0 and 93.9%, respectively (Fig. 3).

For the B adsorption experiment, Stage 1 solution has a B concentration of 5 ± 1 ppb. At 80:1 water:clay ratio, Stage 2 solutions that leached B from leaves combusted at 200, 300 and 550 °C have B concentrations of $68 \pm 7, 336 \pm 34$ and 538 ± 54 ppb, respectively (Fig. 4; Table 1). This corresponds to a gain of 3.2, 16.6, and 26.7 μg of B, respectively. At 30:1 water:clay ratio, the Stage 2 solution have a B concentration of 57 ± 6 ppb, indicating a gain of 2.6 μg of B. After reacting with clays, the B concentrations of Stage 3 solutions for both 30:1 and 80:1 water:clay ratio experiments are within error of those of Stage 2 solutions (Fig. 4).

At 80:1 water:clay ratio, Stage 1 solution has a B isotope composition of $32.90 \pm 0.29‰$. Stage 2 solution that leached leaves combusted at 200 °C has a B isotope composition of $31.38 \pm 0.29‰$, while those of 300 and 550 °C combustion temperatures have $\delta^{11}B$ of $29.19 \pm 0.29‰$ and $29.07 \pm 0.29‰$, respectively (Fig. 4; Table 1). After reacting with clays, Stage 3 solutions of 200 °C combustion temperature show no systematic change in B isotope compositions (Fig. 4). In contrast, those of 300 °C display a systematic increase in $\delta^{11}B$ (by about 1.3‰), while those of 550 °C combustion temperature are characterised by a lighter B isotope composition (by about 1.2‰). At 30:1 water:clay ratio, the Stage 2 solution has the same B isotope composition of $32.90 \pm 0.29‰$ as that of Stage 1 solution. For Stage 3 solution, the $\delta^{11}B$ decreased to ~29‰ (Fig. 4; Table 1).

The soil clay fractions are composed of microcrystalline quartz and kaolinite (Figure S1). For experiments with 80:1 water:clay ratio, they have a B concentration of 18.0 ± 0.7 ppm, and a B isotope composition of $-4.60 \pm 0.29‰$ (Figs. 5). The clays used in the adsorption experiment with 30:1 water:clay ratio has a B concentration of 30.15 ± 0.7 ppm, and the same B isotope composition as those used in the 80:1 water:clay ratio experiments (Table 2). After reacting with Stage 2 leaching solutions of 200, 300 and 550 °C combustion temperature, the B concentration of clays increased by an average of 0.1 ± 1.4, 0.6 ± 1.4 and 2.7 ± 1.4 ppm, respectively (Fig. 5). After reactions at 80:1 water:clay ratio, clays that interacted with solutions from the 200 and 300 °C combustion temperature do not see a significant change in $\delta^{11}B$, while for the 550 °C experiments their B isotope composition increased by a magnitude of ~ 5‰. After reactions at 30:1 water: clay ratio, the B concentration in clay decreased to ~29.2 ppm, while their B isotope compositions show a small increase to an average of ~ −3‰ (Fig. 5; Table 2).

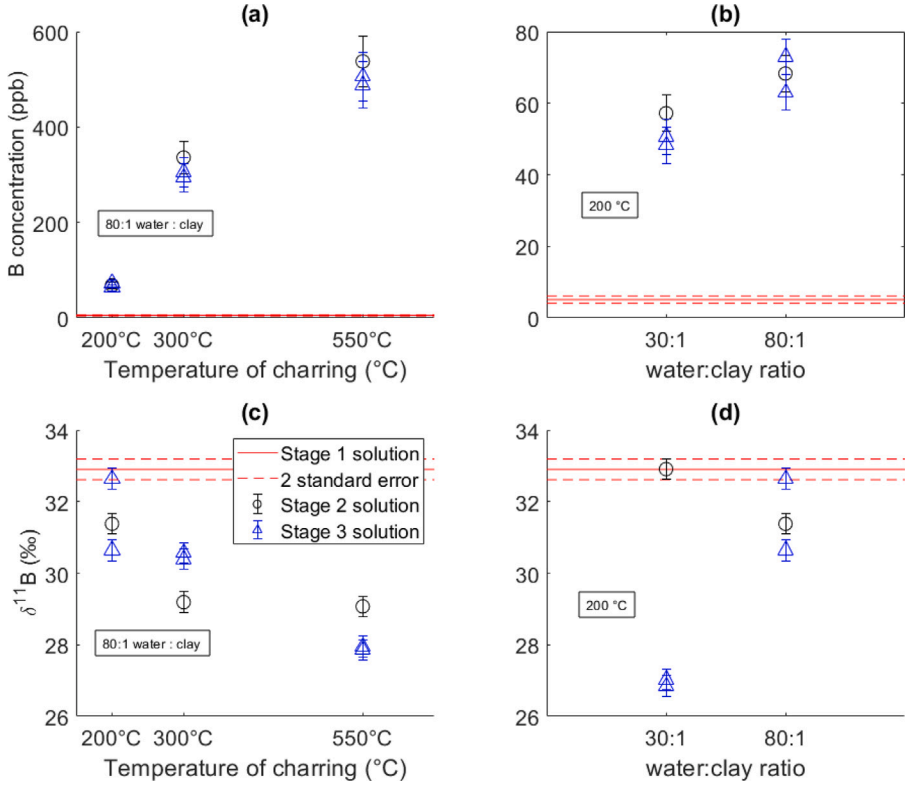

Fig. 4. (a) B concentrations of filtered rainwater (Stage 1 solution), and leaching solutions for eucalypt leaves combusted at various temperatures, before (Stage 2 solution) and after (Stage 3 solution) reacting with clays, at 80:1 water:clay ratio. (b) Comparison of Stage 1, 2 and 3 solutions between 30:1 and 80:1 water:clay ratio experiments that reacted with leaves combusted at 200 °C; (c) B isotope composition of Stage 1, 2 and 3 solutions for combusted eucalypt leaves reacting with clays at 80:1 water:clay ratio; (d) Comparison of B isotope composition of Stage 1, 2 and 3 solutions between 30:1 and 80:1 water:clay ratio experiments that reacted with leaves combusted at 200 °C.

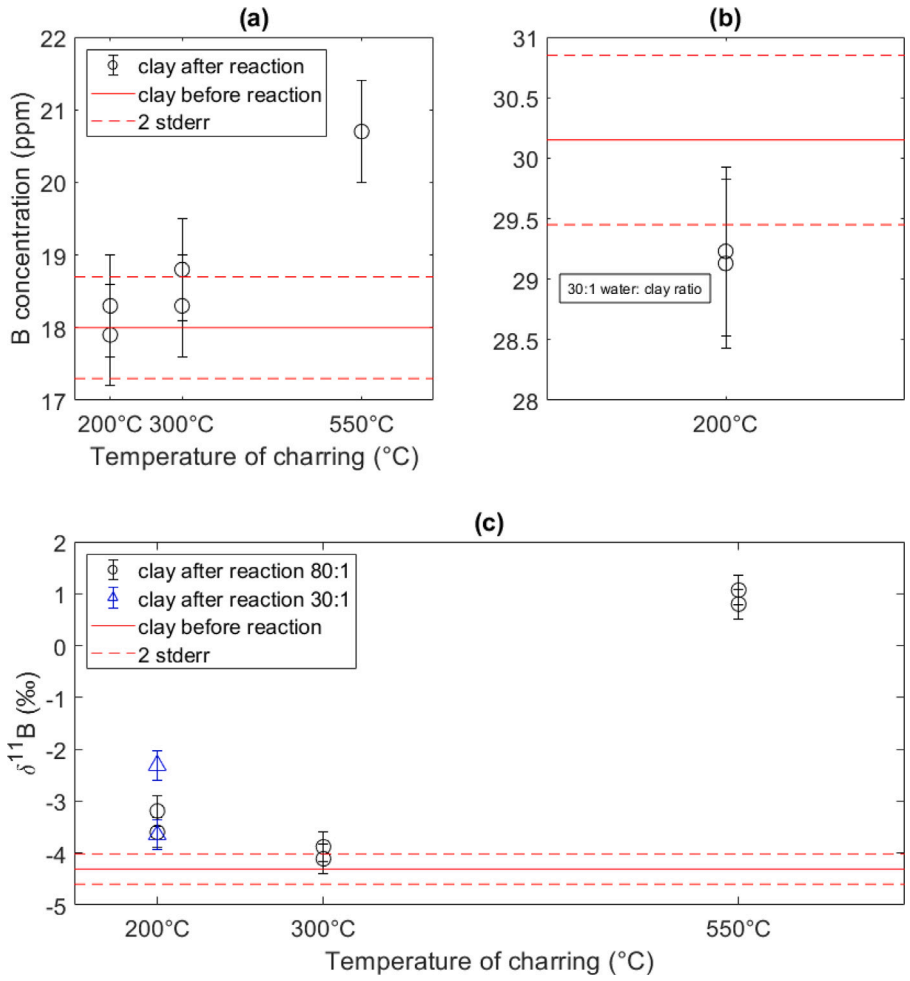

Fig. 5. B concentrations of clays before and after reacting with leaching solutions of eucalypt leaves combusted at various temperatures, at 80:1 (a) and 30:1 (b) water:clay ratio, and their B isotope compositions (c).

4. Discussion

4.1. Plant combustion

The B fraction emitted to the atmosphere during wildfires could be a key factor that influences the B imparted to soil from combusted biomass. If significant amount of isotopically fractionated B is lost through volatilisation, this could change the B isotopic signal in the soil derived from deposition of non-volatilised B. Previous studies have shown that aerosols display higher B concentrations and lighter B isotope compositions during winter in coastal Japan, which was attributed to increased input of lighter B isotopes from coal-burning during winter months (Sakata et al., 2010, 2013). In addition, Chetelat et al. (2005) attributed a decrease of δ^{11}B in rainwater from French Guiana to biomass burning, based on seasonal increase of nitrate concentrations that coincide with decreased δ^{11}B. Analysis of fly ash from two coal-fired power plants in Spain show that 95% of B in coals is retained in ash after combustion (Ochoa-González et al., 2011). In our experiments, we show that the amount of B loss in both eucalypt leaves and bark after combusting at 500 °C is within the 5% uncertainty, which is in agreement with Ochoa-González et al. (2011) (Fig. 2). This suggests that the amount of B released to the atmosphere through volatilisation during wildfires is small compared to the B fraction that is deposited into the soil through ash. However, we also show that the B isotope composition of ash is lighter for both leaves and bark after combustion, indicating that ^{11}B is preferentially volatilised during combustion (Fig. 2). This is in contrast to previous studies which suggested lighter B isotope compositions in atmospheric particulates linked to coal combustion (Chetelat et al., 2005; Sakata et al., 2010, 2013). The contrasting results can possibly be reconciled when considering that atmospheric B can have high δ^{11}B (up to ~20‰) in coastal areas due to B input from evaporated seawater (Chetelat et al., 2005; Sakata et al., 2013). Therefore, the B fraction volatilised during plant combustion could be isotopically lighter than that of the coastal atmosphere, despite the heavier ^{11}B being preferentially volatilised. Assuming a B loss of 5% and B isotope composition change from 32‰ to 29‰ for combusted leaves in a closed system, the δ^{11}B of the volatilised B fraction can be calculated using a mass balance equation:

$$M_l R_l = M_a R_a + M_v R_v \quad (2)$$

where M and R denote the mass of B and ^{11}B/^{10}B ratio, respectively, and subscripts l, a, and v denote fresh leaves, ash and volatilised B fraction, respectively. We calculate that the volatilised B fraction should have a δ^{11}B of 89‰, which is much higher than that of fresh leaves. Thus, our B concentration and isotope composition results suggest that during combustion, a small and highly fractionated B fraction is lost to the atmosphere, resulting in the B fraction deposited in soil being isotopically lighter than the isotope composition of fresh leaves and barks.

4.2. Boron adsorption experiments

4.2.1. Leaching solutions

Rainwater (Stage 1) solutions have an initial pH of around 7. After reacting with combusted leaves, the pH of all Stage 2 solutions

increased (Figs. 6 and 7). The leaching solutions of leaves combusted at 550 °C show the greatest increase in pH. This can be attributed to the higher ash content in the residue combusted at 550 °C (Figs. 3). Carbonates, oxides and hydroxides that make up ash can increase soil pH significantly post-fire (Ulery et al., 1993). Stage 2 leaching solutions of lower combustion temperature experiments all show smaller increases in pH due to less ash being created at low temperatures (Figs. 3). Stage 2 leaching solutions for the combustion experiments at 300 °C have lower pH than those for the 200 °C experiments, which could be due to accelerated humification at higher temperatures (Katsumi et al., 2016). Residue combusted at 200 and 300 °C have similar low ash content, and consist mostly of organics (Figs. 3). Therefore, at this temperature range, humification could be the more important factor for determining pH of leaching solutions. The resulting humic acid could possibly decrease the pH of the solution compared to the leaching solutions of lower combustion temperatures.

After reacting with leaves combusted at 300 and 550 °C, the Stage 2 leaching solutions have a $\delta^{11}B$ of ~ 29‰ (Fig. 4). This is the same B isotope composition as that of leaves ash combusted at 500 °C (Fig. 2), which indicates that there is no isotopic fractionation when B is leached from ash into solution. In contrast, the leaching solutions of leaves combusted at 200 °C has a higher $\delta^{11}B$ of ~ 31.5 and 32.9‰ (for 80:1 and 30:1 water:caly ratio experiments, respectively), which are similar isotope compositions to that of leaves before combustion (Fig. 2). This could suggest that the magnitude of volatilisation is small enough during combustion at 200 °C, such that the combustion residue retains the same B isotope composition as that of fresh leaves, and subsequently imparts the isotopic signal to the leaching solution. Since leaching solutions that reacted with ash combusted at 300 and 550 °C have the same $\delta^{11}B$, it is likely that the amount of volatilisation does not increase linearly with temperature; instead, there is a threshold temperature between 200 and 300 °C, above which significant volatilisation is initiated, and causing measurable B isotope fractionation during the process. Therefore, during low severity fires, if this threshold temperature is not reached, it is possible that B volatilisation would be insignificant, and no B isotope fractionation would have occurred during combustion.

Apart from possibly influencing the magnitude of B volatilisation, combustion temperature likely also affects how plant materials are modified. Stage 2 leaching solutions of combusted leaves have B concentrations that increase approximately linearly with combustion temperature (Fig. 4), suggesting that increased combustion temperature causes B to become more labile. Since increased temperature increasingly degrades organic matter, a possible explanation is that there is less organic matter in combustion residue of higher temperatures (Figs. 3). It is known that B has strong affinity for adsorption onto organic matter (Yermiyahu et al., 2001; Lemarchand et al., 2005). Thus higher organic concentration in residues of leaves combusted at lower temperatures could possibly release less B into solution during leaching. Alternatively, residue combusted at higher temperatures may be more porous and have smaller particle sizes, thus increasing the surface area and the rate of leaching.

After reacting with clay at 80:1 water:clay ratio, Stage 3 solutions show no significant changes to the B concentration (Fig. 4). This could be because the large water:clay ratio does not allow enough B to be adsorbed onto clay to significantly change the B concentration in the solution. During this reaction, the B concentration in clay increased by up to ~ 2.7 ppm (Fig. 5). Considering the mass of clays and solutions, and assuming that no B is lost during the experiment, we can write the following mass balance:

$$M_{si} + M_{ci} = M_{sf} + M_{cf} + M_r \quad (3)$$

where M denotes the mass of B (in ng), and si, sf, ci, cf and r subscripts denote the Stage 2 solution, Stage 3 solution, clay before reaction, clay after reaction, and Stage 4 rinse solution, respectively. Using Eq. (3), we calculate that with a gain of 2.7 ppm of B in

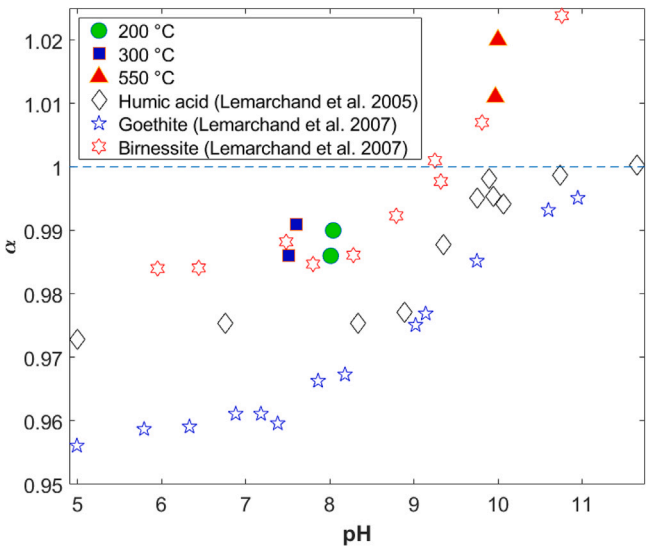

Fig. 6. B isotope fractionation factor (α) for B adsorption onto clays from leaching solutions.

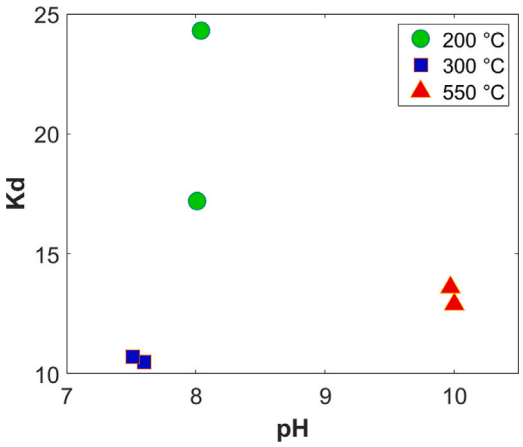

Fig. 7. B partition coefficient (Kd) for B adsorption onto clays from leaching solutions.

0.15 g of clay, and accounting for B desorbed in the rinse solution, the B concentration of leaching solution (with a volume of 12 mL and an initial B concentration of 533 ppb) is expected to decrease by ~ 85 ppb. This calculated change in B concentration of the leaching solutions is within error of our measured decrease of 49 ppb (Fig. 4). Therefore, the water:clay ratio is likely too large to precisely measure changes in B concentration of solutions. After repeating the experiment at a lower water:clay ratio of 30:1 for leaching leaves combusted at 200 °C, we observe that there is a greater difference in the mean B concentration between Stage 2 and 3 solutions, compared to that of experiments performed at larger water:clay ratio (Fig. 4). This suggest that having smaller water:clay ratio does indeed increase the precision of measured changes in B concentration of leaching solutions. However, the B concentration of Stage 2 and 3 solutions are still within error, suggesting that a water:clay ratio even lower than 30:1 would be preferable for precise measurements.

For 80:1 water:clay ratio experiments, a systematic change in the $\delta^{11}B$ of the leaching solutions is not observed after they have reacted with clays (Fig. 4). ^{10}B is generally preferentially adsorbed onto clays (Keren and Mezuman, 1981; Palmer et al., 1987). This should result in an increased $\delta^{11}B$ of solutions after reacting with clays. However, the B isotope fractionation during adsorption can change with

pH (Lemarchand et al., 2005, 2007). We calculate the isotope fractionation factor (α) in our experiments using a Rayleigh distillation formulation:

$$\frac{R_x}{R_o} \approx F^{\alpha-1} \quad (4)$$

where R_o and R_x denotes the $^{11}B/^{10}B$ ratio of the leaching solution before and after reacting with clays, respectively, and F denotes the fraction of B remaining in solution after reacting with clays. For 80:1 water:clay ratio experiments, ^{10}B is preferentially adsorbed onto clays for leaching solutions of leaves combusted at 200 and 300 °C, as indicated by α values < 1, while for those of leaves combusted at 550 °C, ^{11}B is preferentially adsorbed, as indicated by α values > 1 (Fig. 6). This is in agreement with the trends observed in previous studies of B adsorption where α increases dramatically above pH of 9 (Lemarchand et al., 2005, 2007). Therefore, the differences in pH could explain why leaching solutions of leaves combusted at 300 °C increases in $\delta^{11}B$ (preferential ^{10}B adsorption), while those of leaves combusted at 550 °C decreases in $\delta^{11}B$ (preferential ^{11}B adsorption). For B adsorption at neutral to slightly basic pH in our experiments, the $\delta^{11}B$ of adsorbed B is on average about 12‰ lower than that of B in solution (Table 2). For B adsorption at pH of 10, the $\delta^{11}B$ of adsorbed B is on average about 15‰ higher than that of dissolved B (Table 2). The clays in our experiment fractionates B isotopes with pH most similarly to birnessite (a Mn-oxide mineral) (Lemarchand et al., 2007) (Fig. 6). Geothite has greater preference for adsorbing ^{10}B compared to clays in our experiment (Lemarchand et al., 2007) (Fig. 6). It has been suggested that goethite and kaolinite (primary constituent of clays used in this study; Figure S1) form similar inner-sphere complexes when adsorbing B (Goldberg et al., 1993). Thus, it is possible that the type of B complexes formed via ligand exchange during B adsorption is not the sole factor that determines the extent of B isotope fractionation. Surface charge of clay minerals is an important factor for B isotope fractionation during adsorption (Elmaci et al., 2015). Clays tend to have permanent negatively charged sites on the surface, and pH dependent positively or negatively charged sites on Al-OH sites and exposed hydroxyl groups at the edge of the structural layers (Tombácz and Szekeres, 2006). Since different clay minerals have different number of these charged sites, pH can possibly modify the overall surface charge differently, leading to varying B isotope fractionation during adsorption. For 30:1 water:clay ratio experiments, the α values range from 1.033 to 1.049, indicating a preferential adsorption of ^{11}B at pH of ~ 8. This contradicts the B isotope fractionation observed at similar pH for experiments with 80:1 water:clay ratio. This can be reconciled when considering that in the 30:1 water:clay ratio experiments, the clays could be releasing B into solution, rather than just adsorbing B from solution, as inferred by the clays having lower B concentration after reacting with the leaching solutions (Fig. 5). Therefore, the α values calculated using the change in the B isotope compositions of the leaching solutions could be influenced by the B released into solution from the clays, and may not represent the B isotope composition of the B fraction that was adsorbed onto clay surfaces. This also results in the very high $\delta^{11}B$ of adsorbed B calculated using the B isotope compositions of the leaching solutions in the 30:1 water:clay ratio experiments (see Table 1).

4.2.2. Clays

An approximately linear increase of B concentration with combustion temperature is observed in the clay fractions after they have reacted with leaching solutions (Fig. 5). This is likely a result of the increase in B concentration of the leaching solutions with combustion temperature (Fig. 4)- it has been shown that B adsorption is proportional to the B concentration of solution (Goldberg and Forster, 1991; Goldberg, 1997; Lu et al., 2022), thus leaching solutions of higher combustion temperature will have greater B concentration leading to more B adsorption onto clay. Another factor that controls B adsorption is pH. This can be shown with the partition coefficient (Kd), calculated as follows:

$$Kd = \frac{[B]_{ads}}{[B]_{sol}} \quad (5)$$

where $[B]_{ads}$ is the concentration of adsorbed B in clay (in ppb), and $[B]_{sol}$ is the B concentration in solution after reacting with clays (in ppb). The $[B]_{ads}$ can be calculated using the change in B concentration of clays after reacting with the leaching solutions, as well as the B concentration of rinse solutions to account for B removed through desorption. In 80:1 water:clay ratio experiments, we observe maximum adsorption at pH of ~ 8 (Fig. 7). This is in agreement with a previous study that observed a bell-shaped curve with a maximum Kd at pH of 8 for B adsorption onto birnessite and goethite (Lemarchand et al., 2007). This observation can be explained as clay minerals have a greater affinity for $B(OH)_4^-$, which is in greater abundance at increased pH (Keren and Talpaz, 1984). Above pH 8, the Kd decreases again because the surplus of OH^- ions start to compete with $B(OH)_4^-$ for adsorption sites. Despite this trend, clays that reacted with leaching solutions of leaves combusted at 550 °C (pH ~ 10) still experience that greatest B adsorption, indicating that the effects of the increased B concentration in solution may overprint the effects of pH. For 30:1 water:clay ratio experiments, the $[B]_{ads}$ was calculated using the change in B concentration between Stage 2 and 3 solutions instead, as the clays in these experiments had a net loss of B after reacting with the leaching solutions and could not be used to infer the concentration of the adsorbed B fraction. This likely underestimates the amount of adsorbed B, as it does not account for any B released from clay into solution. The Kd values for these experiments range from 3.3 to 5.9, which are low compared to those of 80:1 water:clay ratio experiments. The low Kd value accounts for the possible B exchange between clays and solutions, as the clays were likely both releasing and adsorbing B into and from the leaching solutions, resulting in a smaller net change of B concentration in the solutions. This could be because the clays used in the 30:1 water:clay ratio experiments have much higher B concentration (Fig. 5). In contrast, the clays used in the 80:1 water:clay ratio experiments have a lower B concentration, thus any B released from clays into solution is likely less significant. Despite having different B concentrations, the B isotope composition of clays used in both 80:1 and 30:1 water:clay ratios are the same. The clays used in both 80:1 and 30:1 water:clay ratios were collected from the same site, but at different times (about one year apart). We observe that the B concentration of soil clay fractions can fluctuate through time in nature, possibly with vegetation cycles which dominate the B budget in soil (Fig. 5) (Gaillardet and Lemarchand, 2018). However, the B isotope composition in the soil stayed constant in our sample site (Fig. 5), thus the B concentration fluctuation is not likely caused by artificial contamination. It is possible for B contamination to be introduced through anthropogenic activities (Robinson et al., 2007), and future studies would need to avoid contaminated sites as much as possible.

Clays that reacted with leaching solutions of leaves combusted at 550 °C also show a dramatic increase in $\delta^{11}B$, compared to those that reacted with leaching solutions of leaves combusted at lower temperatures, where only a marginal increase was observed (Fig. 5). Clays before reacting with leaching solutions have a very low $\delta^{11}B$ of ~ −4.2‰, compared to the leaching solutions (Figs. 4). Thus, despite ^{10}B being preferentially adsorbed for 200 and 300 °C combustion temperatures, all clay samples are expected to have increased $\delta^{11}B$ after B adsorption. Clays that reacted with leaching solutions of leaves combusted at 550 °C show a sharp increase in $\delta^{11}B$ due to a combination of increased B adsorption, and greater preference for adsorbing ^{11}B (Figs. 5 and 6). These observations are in contrast to our previous experiment (same author) on eucalypt barks, where a decrease in $\delta^{11}B$ in clays was observed instead after reacting with leaching solutions of higher combustion temperatures (Lu et al., 2022). This can be explained

Table 1
Leaching solutions in B adsorption experiments.

Water:clay ratio	30:1		80:1					
Combustion temperature (in °C)	200	200	200	200	300	300	550	550
Stage 1 pH	7.1	7.1	7.1	7.1	7.1	7.1	7.1	7.1
Stage 1 B concentration (in ppb)	5.1	5.1	5.1	5.1	5.1	5.1	5.1	5.1
Stage 1 δ^{11}B (in ‰)	32.90	32.90	32.90	32.90	32.90	32.90	32.90	32.90
Stage 2 pH	7.7	7.7	7.8	7.8	7.2	7.2	10.9	10.9
Stage 2 B concentration (in ppb)	57	57	68	68	336	336	538	538
Stage 2 δ^{11}B (in ‰)	32.91	32.91	31.38	31.38	29.19	29.19	29.07	29.07
Stage 3 pH	7.8	7.9	8.0	8.0	7.6	7.5	10.0	10.0
Stage 3 B concentration (in ppb)	51	48	63	73	294	306	506	488
Stage 3 δ^{11}B (in ‰)	26.85	27.03	32.64	30.64	30.39	30.57	27.85	27.95
Adsorbed B (ng)	40 ± 6	50 ± 10	160 ± 23	270 ± 38	460 ± 66	500 ± 70	1000 ± 140	1020 ± 140
δ^{11}B of adsorbed B (in ‰)	80 ± 11	64 ± 9.1	17 ± 2.5	20 ± 2.9	21 ± 2.9	15 ± 2.1	49 ± 6.9	40 ± 5.7

The pH, B concentration (in ppb) and B isotope composition (in ‰) of rainwater (Stage 1 solutions), leaching solution of material combusted at different temperatures (Stage 2 solutions), and leaching solutions that subsequently reacted with clay (Stage 3 solutions). Precision is 0.1 for pH (unitless), 10% (2RSE) for the B concentration, and 0.29‰ (2SE) for δ^{11}B of leaching solutions.

Table 2
Soil clay fractions in B adsorption experiments.

Combustion temperature (in °C)	B concentration before reaction (in ppm)	B concentration after reaction (in ppm)	δ^{11}B before reaction (in ‰)	δ^{11}B after reaction (in ‰)	α	$\Delta^{11}B_{ads-sol}$ (in ‰)	Stage 4 solution B concentration (in ppb)
200	18.0	17.9	−4.33	−3.19	0.986 ± 0.020	−14.2	18
200	18.0	18.3	−4.33	−3.60	0.990 ± 0.020	−10.3	23
300	18.0	18.3	−4.33	−3.88	0.991 ± 0.020	−8.8	42
300	18.0	18.8	−4.33	−4.11	0.986 ± 0.020	−14.5	37
550	18.0	20.7	−4.33	1.07	1.020 ± 0.020	19.4	59
550	18.0	20.7	−4.33	0.80	1.011 ± 0.020	11.2	61
200 (30:1)	30.2	29.2	−4.33	−2.31	1.049 ± 0.020	47.4	–
200 (30:1)	30.2	29.1	−4.33	−3.65	1.033 ± 0.020	32.9	–

The B concentration (in ppm) and δ^{11}B of soil clay fractions before and after reacting with Stage 2 leaching solutions, the isotope fractionation factor (α) of B adsorption onto clays from leaching solutions, the isotope fractionation between adsorbed and dissolved B ($\Delta^{11}B_{ads-sol}$), and the B concentration (in ppb) of Stage 4 rinse solutions.

as bark has lower δ^{11}B than leaves (Fig. 2), due to xylem sap becoming more enriched in ^{11}B the further from the roots (Roux et al., 2022). Since an increase of δ^{11}B was observed in soil clay fractions of Yengo National Park (NSW, Australia) after experiencing higher severity fires, it was hypothesised that the B isotope composition of soil clay fractions after wildfires is controlled by the amount of leaves combusted (Lu et al., 2022). Our experiments here support this hypothesis, as experimentally combusted leaves can replicate the increased δ^{11}B in clays as observed in Yengo National Park soil samples.

The adsorbed B in our 80:1 water:clay ratio experiments displays hysteresis, as not all adsorbed B is desorbed during rinsing, leading to increase of B concentration and δ^{11}B in clays (Figs. 5). This would suggest the formation of inner-sphere B complexes, which are not as easily desorbed as outer-sphere complexes. Goldberg et al. (1993) had previously suggested inner-sphere complex formation as the dominant mode of B adsorption for kaolinite, based on calculations of ionic strength dependence and zero point charge results. However, since a large portion of adsorbed B was desorbed after clays were rinsed once in our experiment (Table 2), it is possible that multiple species of B complexes were formed during adsorption, only some of which were hysteretic. It is unclear if this hysteretic B fraction represents a permanent gain of B. Goldberg and Suarez (2012) found that a time frame of months to years may be required for adsorbed B to be exhibit hysteresis. Thus, it is possible that repeated rinsing could have removed even inner-sphere B complexes, as our reaction time was only 15 h. In our 30:1 water:clay ratio experiments, the clays have a net loss of B after reacting with leaching solutions, indicating that more B was desorbed during rinsing than was adsorbed. The clays in these experiments have a higher initial B concentration, which could suggest that a significant amount of B was already adsorbed onto their surfaces from soil solution prior to our experiments. During rinsing, the initial adsorbed B could be lost in addition to any B adsorbed from our leaching solutions, leading to a net loss of B. In nature, drying and wetting cycles increase the hysteresis of B adsorbed onto clays (Keren and Gast, 1981). Therefore, the adsorbed B fraction in our experiments is possibly only weakly hysteretic, as the reaction involved neither long durations, nor wetting and drying cycles. In natural wildfires, it is likely that the deposited ash persists long enough in the soil to achieve a stronger hysteresis, as the relationship between combustion and B isotope signal in clays had been observed in stream sediments (Ryan et al., 2023), which would not be possible if the adsorption were easily reversible.

4.3. Implications

Boron isotopes in atmospheric particulates can be useful in tracking fossil fuel burning, as coals tend to have low δ^{11}B. Previous studies assume that this light B isotope composition is transferred to atmospheric particulates during volatilisation without any isotopic fractionation (Sakata et al., 2010, 2013). However, our experiments show that isotopic fractionation does occur with a temperature threshold between 200 and 300 °C during combustion and volatilisation, where ^{11}B is preferentially volatilised. Though this likely does not affect trends from coastal sites, due to the heavy background B isotope composition of

aerosols linked to seawater, it should be accounted for in more inland studies where the preferential loss of ^{11}B may mask coal burning. For wildfires, this isotope fractionation during combustion does not preclude a B isotope signal being imparted in the soil, as the isotope fractionation is small, and leaves tend to have much higher $\delta^{11}B$ compared to soil minerals. Though we observe that pH, B concentration and water:clay ratio can all influence B isotope fractionation during adsorption onto clay minerals, we were able to replicate the increased $\delta^{11}B$ in clays following high severity fires observed in previous studies, by reacting clays with leaching solutions of combusted leaves (Fig. 5). This shows that B isotope signals following wildfires is likely a function of the amount of combusted leaves (and by extension flame height). Although wildfires can consume different material with different B isotope compositions, the variations in the B isotope compositions imparted to soil is likely determined by combustion of leaves on tall trees, as shorter plants would be consumed in both low and high severity fires. This signal has been shown to persist in stream sediments (Ryan et al., 2023), thus it may be possible to reconstruct a fire severity history by studying boron isotopes in sediment sequences. This would be invaluable, as only fire occurrence histories are currently available, and it is difficult to infer if wildfires are becoming more severe in addition to becoming more frequent due to climate change. Additionally, while burning leaves increases the $\delta^{11}B$ of clays, combustion of lower plant compartments such as bark can decrease the $\delta^{11}B$ of clays instead. Peltola and Åström (2006) found a decrease of $\delta^{11}B$ in lake sediments linked to a historic town fire. This can be explained as a town fire combusts only wood, which have lower $\delta^{11}B$ than leaves. Therefore, it may be possible to differentiate wood fires from wildfires in the B isotope signals, and perhaps a record of man-made fires by early human civilisations can also be inferred with this new proxy.

5. Conclusions

Boron isotopes are fractionated during plant combustion, where ^{11}B is preferentially volatilised. The volatilised B fraction is small (< 5% of total B). Boron in ash of combusted eucalypt leaves have higher $\delta^{11}B$ (29.06 ±0.29‰) than that of combusted eucalypt barks bark (6.51 ±0.29‰), due to intra-plant B isotope fractionation. Rainwater leach B from ash of combusted leaves that can be adsorbed onto clay minerals in the soil and increase the $\delta^{11}B$ of clays by up to 5‰. This increase of B isotope composition in clays is comparable to that observed in soils that experienced a high severity fire, thus suggesting that leaf combustion is a key factor in determining the B isotope composition of soil following fires. It is therefore possible to differentiate wildfire severity using B isotopes based on the proportion of leaves combusted. Ash from combusted leaves can change the pH of leaching solutions, which in turn controls the amount of B adsorption, and the B isotope fractionation during adsorption. Though ^{10}B is usually favoured during B adsorption onto clay minerals, it is possible for ^{11}B to be preferentially adsorbed at high pH. Thus, the temperature of wildfires is also important, as it affects ash production and therefore soil pH. Boron adsorption onto clays displays a degree of hysteresis, suggesting that the relationship between combustion and B signal in clays can be preserved for long durations.

CRediT authorship contribution statement

Shawn Lu: Conceptualization, Data curation, Formal analysis, Investigation, Methodology, Writing – original draft, Writing – review & editing. **Anthony Dosseto:** Funding acquisition, Project administration, Resources, Supervision. **Damien Lemarchand:** Supervision.

Declaration of competing interest

The authors declare that they have no known competing financial interests or personal relationships that could have appeared to influence the work reported in this paper.

Data availability

Data are available through Mendeley Data at https://doi.org/10.17632/tgd5kj3wzk.2.

Acknowledgements

The authors would like to thank Bach Tran, from the Faculty of Engineering and Information Sciences at the University of Wollongong, for his assistance with X-ray diffraction analysis for this study. This work was funded by the Australian Research Council (Grant number: DP200101123).

Appendix A. Supplementary data

The Supplementary Material section contains B isotope and concentration data for the B leaching and adsorption experiments, as well as for eucalypt barks and leaves. The XRD spectrum of the clay used in the B adsorption experiment is also included here in graphic form, while the spectral data can be found in the data package (as described in the Data Availability section).

Supplementary material related to this article can be found online at https://doi.org/10.1016/j.gca.2024.04.024.

References

Blevins, D.G., Lukaszewski, K.M., 1998. Boron in plant structure and function. Ann. Rev. Plant Biol. 49 (1), 481–500.

Buoso, S., Pagliari, L., Musetti, R., Fornasier, F., Martini, M., Loschi, A., Fontanella, M.C., Ermacora, P., 2020. With or without you: Altered plant response to boron-deficiency in hydroponically grown grapevines infected by grapevine pinot gris virus suggests a relation between grapevine leaf mottling and deformation symptom occurrence and boron plant availability. Front. Plant Sci. 11, http://dx.doi.org/10.3389/fpls.2020.00226, URL: https://www.frontiersin.org/article/10.3389/fpls.2020.00226.

Chen, Z., Hu, Z., Peng, J., Sun, A., Yan, L., Xu, Q., 2023. Boron isotopic fractionation in Brassica napus L. plants during plant growth under hydroponic conditions. Plant Soil http://dx.doi.org/10.1007/s11104-022-05839-x.

Chetelat, B., Gaillardet, J., Freydier, R., Négrel, P., 2005. Boron isotopes in precipitation: experimental constraints and field evidence from French Guiana. Earth Planet. Sci. Lett. 235 (1–2), 16–30.

Cividini, D., Lemarchand, D., Chabaux, F., Boutin, R., Pierret, M.-C., 2010. From biological to lithological control of the B geochemical cycle in a forest watershed (Strengbach, Vosges). Geochim. Cosmochim. Acta 74 (11), 3143–3163. http://dx.doi.org/10.1016/j.gca.2010.03.002, URL: https://www.sciencedirect.com/science/article/pii/S001670371000116X.

Cox, J.A., Lundquist, G.L., Przyjazny, A., Schmulbach, C.D., 1978. Leaching of boron from coal ash. Environ. Sci. Technol. 12 (6), 722–723.

Dembitsky, V.M., Smoum, R., Al-Quntar, A.A., Ali, H.A., Pergament, I., Srebnik, M., 2002. Natural occurrence of boron-containing compounds in plants, algae and microorganisms. Plant Sci. 163 (5), 931–942. http://dx.doi.org/10.1016/S0168-9452(02)00174-7, URL: https://www.sciencedirect.com/science/article/pii/S0168945202001747.

Elmaci, G., Icten, O., Ay, A.N., Zümreoglu-Karan, B., 2015. Boron isotopic fractionation in aqueous boric acid solutions over synthetic minerals: Effect of layer and surface charge on fractionation factor. Appl. Clay Sci. 107, 117–121. http://dx.doi.org/10.1016/j.clay.2015.01.011, URL: https://www.sciencedirect.com/science/article/pii/S0169131715000198.

Ercolani, C., Lemarchand, D., Dosseto, A., 2019. Insights on catchment-wide weathering regimes from boron isotopes in riverine material. Geochim. Cosmochim. Acta 261, 35–55. http://dx.doi.org/10.1016/j.gca.2019.07.002, URL: https://www.sciencedirect.com/science/article/pii/S0016703719304120.

Gaillardet, J., Lemarchand, D., 2018. Boron in the weathering environment. In: Boron Isotopes. Springer, pp. 163–188.

Gangjian, W., Jingxian, W., Ying, L., Ting, K., Zhongyuan, R., Jinlong, M., Yigang, X., 2013. Measurement on high-precision boron isotope of silicate materials by a single column purification method and MC-ICP-MS. J. Anal. At. Spectrom. 28, 606–612. http://dx.doi.org/10.1039/C3JA30333K.

Geilert, S., Vogl, J., Rosner, M., Eichert, T., 2019. Boron isotope variability related to boron speciation (change during uptake and transport) in bell pepper plants and SI traceable n (11B)/n (10B) ratios for plant reference materials. Rapid Commun. Mass Spectrom. 33 (13), 1137–1147.

Geilert, S., Vogl, J., Rosner, M., Voerkelius, S., Eichert, T., 2015. Boron isotope fractionation in bell pepper. Mass Spectrom. Purif. Techn. 1 (101), http://dx.doi.org/10.4172/2469-9861.1000101, URL: https://oceanrep.geomar.de/id/eprint/30548/.

Goldberg, S., 1997. Reactions of boron with soils. Plant Soil 193, 35–48. http://dx.doi.org/10.1023/A:1004203723343.

Goldberg, S., Forster, H.S., 1991. Boron sorption on calcareous soils and reference calcites. Soil Sci. 152, 304–310.

Goldberg, S., Forster, H.S., Heick, E.L., 1993. Boron adsorption mechanisms on oxides, clay minerals, and soils inferred from ionic strength effects. Soil Sci. Am. J. 57 (3), 704–708. http://dx.doi.org/10.2136/sssaj1993.03615995005700030013x, arXiv:https://acsess.onlinelibrary.wiley.com/doi/pdf/10.2136/sssaj1993.03615995005700030013x. URL: https://acsess.onlinelibrary.wiley.com/doi/abs/10.2136/sssaj1993.03615995005700030013x.

Goldberg, S., Suarez, D.L., 2012. Role of organic matter on boron adsorption-desorption hysteresis of soils. Soil Sci. 177, 417–423. http://dx.doi.org/10.1097/SS.0b013e318256bc0c.

Govindaraju, K., 1994. 1994 Compilation of working values and sample description for 383 geostandards. Geostandards Newsletter 18 (S1), 1–158. http://dx.doi.org/10.1046/j.1365-2494.1998.53202081.x-i1, arXiv:https://onlinelibrary.wiley.com/doi/pdf/10.1046/j.1365-2494.1998.53202081.x-i1. URL: https://onlinelibrary.wiley.com/doi/abs/10.1046/j.1365-2494.1998.53202081.x-i1.

Hollis, J.F., Keren, R., Gal, M., 1988. Boron release and sorption by fly ash as affected by pH and particle size. J. Environ. Qual. 17 (2), 181–184. http://dx.doi.org/10.2134/jeq1988.00472425001700020002x, arXiv:https://acsess.onlinelibrary.wiley.com/doi/pdf/10.2134/jeq1988.00472425001700020002x. URL: https://acsess.onlinelibrary.wiley.com/doi/abs/10.2134/jeq1988.00472425001700020002x.

Hu, Z., Gao, S., 2008. Upper crustal abundances of trace elements: A revision and update. Chem. Geol. 253 (3), 205–221. http://dx.doi.org/10.1016/j.chemgeo.2008.05.010, URL: https://www.sciencedirect.com/science/article/pii/S000925410800185X.

Kakihana, H., Kotaka, M., Satoh, S., Nomura, M., Okamoto, M., 1977. Fundamental studies on the ion-exchange separation of boron isotopes. Bull. Chem. Soc. Jpn. 50 (1), 158–163. http://dx.doi.org/10.1246/bcsj.50.158.

Katsumi, N., Yonebayashi, K., Okazaki, M., 2016. Effects of heating on composition, degree of darkness, and stacking nanostructure of soil humic acids. Sci. Total Environ. 541, 23–32. http://dx.doi.org/10.1016/j.scitotenv.2015.09.012, URL: https://www.sciencedirect.com/science/article/pii/S0048969715306720.

Keren, R., Gast, R.G., 1981. Effects of wetting and drying, and of exchangeable cations, on boron adsorption and release by montmorillonite. Soil Sci. Am. J. 45 (3), 478–482. http://dx.doi.org/10.2136/sssaj1981.03615995004500030007x, arXiv:https://acsess.onlinelibrary.wiley.com/doi/pdf/10.2136/sssaj1981.03615995004500030007x. URL: https://acsess.onlinelibrary.wiley.com/doi/abs/10.2136/sssaj1981.03615995004500030007x.

Keren, R., Mezuman, U., 1981. Boron adsorption by clay minerals using a phenomenological equation. Clays Clay Miner. 29, 198–204. http://dx.doi.org/10.1346/CCMN.1981.0290305.

Keren, R., Talpaz, H., 1984. Boron adsorption by montmorillonite as affected by particle size. Soil Sci. Am. J. 48 (3), 555–559. http://dx.doi.org/10.2136/sssaj1984.03615995004800030017x, arXiv:https://acsess.onlinelibrary.wiley.com/doi/pdf/10.2136/sssaj1984.03615995004800030017x. URL: https://acsess.onlinelibrary.wiley.com/doi/abs/10.2136/sssaj1984.03615995004800030017x.

Kot, F.S., Farran, R., Fujiwara, K., Kharitonova, G.V., Kochva, M., Shaviv, A., Sugo, T., 2016. On boron turnover in plant–litter–soil system. Geoderma 268, 139–146. http://dx.doi.org/10.1016/j.geoderma.2016.01.022, URL: https://www.sciencedirect.com/science/article/pii/S0016706116300234.

Lemarchand, D., Cividini, D., Turpault, M.-P., Chabaux, F., 2012. Boron isotopes in different grain size fractions: Exploring past and present water–rock interactions from two soil profiles (Strengbach, Vosges Mountains). Geochim. Cosmochim. Acta 98, 78–93.

Lemarchand, E., Schott, J., Gaillardet, J., 2005. Boron isotopic fractionation related to boron sorption on humic acid and the structure of surface complexes formed. Geochim. Cosmochim. Acta 69 (14), 3519–3533. http://dx.doi.org/10.1016/j.gca.2005.02.024, URL: https://www.sciencedirect.com/science/article/pii/S0016703705001717.

Lemarchand, E., Schott, J., Gaillardet, J., 2007. How surface complexes impact boron isotope fractionation: Evidence from Fe and Mn oxides sorption experiments. Earth Planet. Sci. Lett. 260 (1), 277–296. http://dx.doi.org/10.1016/j.epsl.2007.05.039, URL: https://www.sciencedirect.com/science/article/pii/S0012821X07003469.

Lu, S., Dosseto, A., Lemarchand, D., Dlapa, P., Simkovic, I., Bradstock, R., 2022. Investigating boron isotopes and FTIR as proxies for bushfire severity. Catena 219, 106621. http://dx.doi.org/10.1016/j.catena.2022.106621, URL: https://www.sciencedirect.com/science/article/pii/S0341816222006075.

Mengel, K., Kirkby, E.A., Kosegarten, H., Appel, T., 2001. Boron. In: Principles of Plant Nutrition. Springer Netherlands, Dordrecht, pp. 621–638.

Miwa, K., Fujiwara, T., 2010. Boron transport in plants: co-ordinated regulation of transporters. Ann. Botany 105 (7), 1103–1108. http://dx.doi.org/10.1093/aob/mcq044, arXiv:https://academic.oup.com/aob/article-pdf/105/7/1103/16999606/mcq044.pdf.

Ochoa-González, R., Cuesta, A.F., Córdoba, P., Díaz-Somoano, M., Font, O., López-Antón, M.A., Querol, X., Martínez-Tarazona, M.R., Giménez, A., 2011. Study of boron behaviour in two spanish coal combustion power plants. J. Environ. Manag. 92 (10), 2586–2589. http://dx.doi.org/10.1016/j.jenvman.2011.05.028, URL: https://www.sciencedirect.com/science/article/pii/S0301479711001836.

Palmer, M., Spivack, A., Edmond, J., 1987. Temperature and pH controls over isotopic fractionation during adsorption of boron on marine clay. Geochim. Cosmochim. Acta 51 (9), 2319–2323. http://dx.doi.org/10.1016/0016-7037(87)90285-7, URL: https://www.sciencedirect.com/science/article/pii/0016703787902857.

Peltola, P., Åström, M., 2006. Can boron and boron isotopes be used as a sedimentary marker for fire events? A case study from a historic urban fire event in W Finland. Appl. Geochem. 21 (6), 941–948. http://dx.doi.org/10.1016/j.apgeochem.2006.01.005, URL: https://www.sciencedirect.com/science/article/pii/S088329270600028X.

Robinson, B., Green, S., Chancerel, B., Mills, T., Clothier, B., 2007. Poplar for the phytomanagement of boron contaminated sites. Environ. Pollut. 150 (2), 225–233. http://dx.doi.org/10.1016/j.envpol.2007.01.017, URL: https://www.sciencedirect.com/science/article/pii/S0269749107000590.

Roux, P., Lemarchand, D., Hughes, H.J., Turpault, M.-P., 2015. A rapid method for determining boron concentration (ID-ICP-MS) and δ11B (MC-ICP-MS) in vegetation samples after microwave digestion and cation exchange chemical purification. Geostandards Geoanal. Res. 39 (4), 453–466. http://dx.doi.org/10.1111/j.1751-908X.2014.00328.x, arXiv:https://onlinelibrary.wiley.com/doi/pdf/10.1111/j.1751-908X.2014.00328.x.

Roux, P., Lemarchand, D., Redon, P.-O., Turpault, M.-P., 2022. B and δ11B biogeochemical cycle in a beech forest developed on a calcareous soil: Pools, fluxes, and forcing parameters. Sci. Total Environ. 806, 150396. http://dx.doi.org/10.1016/j.scitotenv.2021.150396, URL: https://www.sciencedirect.com/science/article/pii/S0048969721054735.

Ryan, R., Dosseto, A., Lemarchand, D., Dlapa, P., Thomas, Z., Simkovic, I., Bradstock, R., 2023. Boron isotopes and FTIR spectroscopy to identify past high severity fires. Catena 222, 106887. http://dx.doi.org/10.1016/j.catena.2022.106887, URL: https://www.sciencedirect.com/science/article/pii/S0341816222008736.

Sakata, M., Ishikawa, T., Mitsunobu, S., 2013. Effectiveness of sulfur and boron isotopes in aerosols as tracers of emissions from coal burning in Asian continent. Atmos. Environ. 67, 296–303. http://dx.doi.org/10.1016/j.atmosenv.2012.11.025, URL: https://www.sciencedirect.com/science/article/pii/S1352231012010874.

Sakata, M., Natsumi, M., Tani, Y., 2010. Isotopic evidence of boron in precipitation originating from coal burning in Asian continent. GEOCHEMICAL JOURNAL 44 (2), 113–123. http://dx.doi.org/10.2343/geochemj.1.0049.

Schlesinger, W.H., Vengosh, A., 2016. Global boron cycle in the Anthropocene. Glob. Biogeochem. Cycles 30 (2), 219–230.

Starkey, H.C., Blackmon, P.D., Hauff, P.L., 1984. The routine mineralogical analysis of clay-bearing samples. Bulletin 1563, http://dx.doi.org/10.3133/b1563.

Tombácz, E., Szekeres, M., 2006. Surface charge heterogeneity of kaolinite in aqueous suspension in comparison with montmorillonite. Appl. Clay Sci. 34 (1), 105–124. http://dx.doi.org/10.1016/j.clay.2006.05.009, URL: https://www.sciencedirect.com/science/article/pii/S0169131706001232. Layer Charge of Clay Minerals.

Ulery, A.L., Graham, R.C., Amrhein, C., 1993. Wood-ash composition and soil pH following intense burning. Soil Sci. 156 (5), 358–364. http://dx.doi.org/10.1097/00010694-199311000-00008.

Vogl, J., Rosner, M., 2012. Production and certification of a unique set of isotope and delta reference materials for boron isotope determination in geochemical, environmental and industrial materials. Geostandards Geoanal. Res. 36 (2), 161–175. http://dx.doi.org/10.1111/j.1751-908X.2011.00136.x, arXiv:https://onlinelibrary.wiley.com/doi/pdf/10.1111/j.1751-908X.2011.00136.x.

Wright, C.C., Wooton, K.M., Twiss, K.C., Newman, E.T., Rasbury, E.T., 2021. Boron isotope analysis reveals borate selectivity in seaweeds. Environ. Sci. Technol. 55 (18), 12724–12730.

Xiao, J., Vogl, J., Rosner, M., Jin, Z., 2022. Boron isotope fractionation in soil-plant systems and its influence on biogeochemical cycling. Chem. Geol. 606, 120972. http://dx.doi.org/10.1016/j.chemgeo.2022.120972, URL: https://www.sciencedirect.com/science/article/pii/S0009254122002662.

Yermiyahu, U., Keren, R., Chen, Y., 2001. Effect of composted organic matter on boron uptake by plants. Soil Sci. Am. J. 65 (5), 1436–1441. http://dx.doi.org/10.2136/sssaj2001.6551436x, arXiv:https://acsess.onlinelibrary.wiley.com/doi/pdf/10.2136/sssaj2001.6551436x. URL: https://acsess.onlinelibrary.wiley.com/doi/abs/10.2136/sssaj2001.6551436x.